

# Seven-Tesla Magnetization Transfer Imaging to Detect Multiple Sclerosis White Matter Lesions

I-Jun Chou, Su-Yin Lim, Radu Tanasescu, Ali Al-Radaideh, Olivier E. Mouglin, Christopher R. Tench, William P. Whitehouse, Penny A. Gowland, Cris S. Constantinescu

From the Division of Clinical Neuroscience (I-JC, S-YL, RT, CRT, CSC); Division of Academic Child Health (I-JC, WPW), School of Medicine, University of Nottingham, Nottingham, UK; Division of Paediatric Neurology, Chang Gung Memorial Hospital, Taoyuan, Taiwan (I-JC); Department of Neurology, Neurosurgery and Psychiatry, Carol Davila University of Medicine and Pharmacy, Colentina Hospital, Bucharest, Romania (RT); Sir Peter Mansfield Magnetic Resonance Centre, School of Physics and Astronomy, University of Nottingham, England, UK (AA-R, OEM, PAG); and Department of Medical Imaging, Faculty of Allied Health Sciences, Hashemite University, Zarqa, Jordan (AA-R).

## ABSTRACT

**BACKGROUND AND PURPOSE:** Fluid-attenuated inversion recovery (FLAIR) imaging at 3 Tesla (T) field strength is the most sensitive modality for detecting white matter lesions in multiple sclerosis. While 7T FLAIR is effective in detecting cortical lesions, it has not been fully optimized for visualization of white matter lesions and thus has not been used for delineating lesions in quantitative magnetic resonance imaging (MRI) studies of the normal appearing white matter in multiple sclerosis. Therefore, we aimed to evaluate the sensitivity of 7T magnetization-transfer-weighted ( $MT_w$ ) images in the detection of white matter lesions compared with 3T-FLAIR.

**METHODS:** Fifteen patients with clinically isolated syndrome, 6 with multiple sclerosis, and 10 healthy participants were scanned with 7T 3-dimensional (D)  $MT_w$  and 3T-2D-FLAIR sequences on the same day. White matter lesions visible on either sequence were delineated.

**RESULTS:** Of 662 lesions identified on 3T-2D-FLAIR images, 652 were detected on 7T-3D- $MT_w$  images (sensitivity, 98%; 95% confidence interval, 97% to 99%). The Spearman correlation coefficient between lesion loads estimated by the two sequences was .910. The intrarater and interrater reliability for 7T-3D- $MT_w$  images was good with an intraclass correlation coefficient (ICC) of 98.4% and 81.8%, which is similar to that for 3T-2D-FLAIR images (ICC 96.1% and 96.7%).

**CONCLUSION:** Seven-Tesla  $MT_w$  sequences detected most of the white matter lesions identified by FLAIR at 3T. This suggests that 7T- $MT_w$  imaging is a robust alternative for detecting demyelinating lesions in addition to 3T-FLAIR. Future studies need to compare the roles of optimized 7T-FLAIR and of 7T- $MT_w$  imaging.

**Keywords:** Demyelination, FLAIR, magnetization transfer-saturated sequence, multiple sclerosis.

**Acceptance:** Received June 4, 2017, and in revised form August 17, 2017. Accepted for publication August 18, 2017.

**Correspondence:** Address correspondence to Cris S. Constantinescu, Clinical Neurology Research Group, Division of Clinical Neuroscience, School of Medicine, University of Nottingham, Queen's Medical Centre, Nottingham NG7 2UH, UK. Email: cris.constantinescu@nottingham.ac.uk.

**Acknowledgments and disclosure:** This work was funded by the Medical Research Council, the Chang Gung Memorial Hospital (project CM-RPG4A0124), the European Neurological Society, and the University of Nottingham. The sponsors of the study had no role in design and conduct of the study; collection, management, analysis, and interpretation of the data; and preparation, review, or approval of the manuscript. The authors have no conflicts of interest to declare.

J Neuroimaging 2017;00:1-8.

DOI: 10.1111/jon.12474

## Introduction

Multiple sclerosis (MS) is a chronic debilitating disease with a prevalence of 203 cases per 100,000 population in the UK.<sup>1</sup> After the first attack (clinically isolated syndrome [CIS]), more than 85% of adult-onset patients experience a relapsing-remitting MS course (RRMS) and 10% have a primary progressive MS.<sup>2</sup> Magnetic resonance imaging (MRI) is regarded as an essential tool for lesion identification and diagnosis,<sup>3</sup> estimation of lesion load and disease activity,<sup>4</sup> and prediction of disease outcomes.<sup>5</sup> Proton-density-weighted imaging has traditionally been used to detect MS lesions. Magnetization transfer (MT) sensitizes MR images to the effect of exchange with macromolecules by off-resonance saturation.<sup>6</sup> MT is sensitive to the integrity of the white matter, due to proton exchange with macromolecules in myelin.<sup>7,8</sup> Often, MT ratio (MTR) maps are used to improve specificity to MT effects and these are made by comparing standard images with MT-weighted ( $MT_w$ )

images. However, raw  $MT_w$  images have greater sensitivity than processed MTR maps, because they retain some sensitivity to other contrasts. Here,  $MT_w$  images are used for lesion detection, rather than lesion characterization. On  $MT_w$  images, abnormal tissue with low myelination is hyperintense with respect to the surrounding white matter tissue. Dousset et al applied  $MT_w$  imaging to characterize white matter lesions in MS and its animal model.<sup>9</sup> Pathological correlation studies show that MT changes reflect decreased myelin content, due to demyelination or incomplete remyelination.<sup>10</sup> Waesberghe et al showed better MS lesion delineation using  $MT_w$  compared to traditional proton-density images and the number of lesions was equal.<sup>11</sup> MT imaging can monitor both demyelination and remyelination in patients with MS.<sup>12</sup>

T2-weighted techniques are sensitive for detecting demyelinating lesions because brain tissue with increased water content appears hyperintense. T2 fluid-attenuated inversion recovery

This is an open access article under the terms of the Creative Commons Attribution-NonCommercial License, which permits use, distribution and reproduction in any medium, provided the original work is properly cited and is not used for commercial purposes.

(FLAIR) imaging, an inversion recovery sequence with long T1 to suppress signal from free water (ie, free water appears dark), is superior to simple T2-weighted imaging for delineating the interface between cerebrospinal fluid (CSF) (free water) and normal brain tissue.<sup>13</sup> It is sensitive to tissue abnormalities including inflammation, edema, demyelination, axonal loss, and gliosis.<sup>14</sup> However, in FLAIR, the detection of brainstem MS lesions is inferior to T2-weighted imaging because of artifacts from CSF flow.<sup>15</sup> Current clinical guidelines recommend using T2-FLAIR imaging at 1.5T or 3T to detect lesions in MS patients, especially in the supratentorial region.<sup>16</sup>

At 7T, MT with submilliliter imaging resolution enables detection of MS cortical lesions<sup>17</sup> and improves quantitative assessment of nonlesional “normal appearing” brain tissue.<sup>18</sup> Therefore, 7T MT provides high-resolution information on myelin integrity.

Currently, FLAIR at 7T has the potential to characterize white matter lesions in MS; however, the sensitivity of lesion counts remains challenging. De Graaf et al compared 3-dimensional (D) FLAIR between 7T and 3T, showing that white matter lesion counts were higher at 3T, although cortical lesion counts were higher at 7T.<sup>19</sup> Thus, studies showing the superiority of 7T FLAIR are largely restricted to detect cortical rather than white matter lesions.<sup>19,20</sup> To achieve better white matter lesion detection in FLAIR at 7T, magnetization-prepared 3D-FLAIR has been developed<sup>21,22</sup> and optimized.<sup>23</sup> It requires tailored radiofrequency (RF) pulses to alleviate inhomogeneities inside the RF transmit field while keeping within specific absorption rate (SAR) constraints, unavailable to us at the time of this study. To our knowledge, lesion-wise comparison of white matter MS lesions between magnetization-prepared 3D-FLAIR at 7T and FLAIR at 3T has not yet been performed.

As the ability to acquire optimized FLAIR imaging at 7T as described by Saranatan and colleagues<sup>23</sup> to detect MS white matter lesions was lacking at the time of our study, and as 7T FLAIR images obtained without RF optimization provided unsatisfactory contrast for white matter lesion detection (see Results section), here we used 3T images instead. Patients participating in a 7T MT imaging MRI research study underwent 3T-FLAIR imaging, on the same day.<sup>18</sup> The hypothesis of the study was that the lesion detection rate of supratentorial white matter in patients with MS is similar between 7T MT<sub>w</sub> and 3T FLAIR.

## Methods

### Patients

Fifteen patients with CIS, 6 with MS, and 10 healthy participants were recruited. Patients were assessed with the Expanded Disability Status Scale (EDSS),<sup>24</sup> Fatigue Severity Scale (FSS),<sup>25</sup> and Multiple Sclerosis Functional Composite (MSFC)<sup>26</sup> by a neurologist (SYL). Patients were recruited from the MS Clinic, University Hospitals Nottingham NHS Trust. This study was approved by the local Research Ethics Committee (REC reference 07/H0408/115). Participants gave written informed consent.

### MR Imaging

Participants underwent MRI in the Sir Peter Mansfield Imaging Centre (SPMIC) using a 7T Philips Achieva scanner (Philips Medical Systems, Best, the Netherlands). The

scanner is equipped with whole-body gradients, a 16-channel head-only receive coil, and a head-only volume quadrature transmit RF coil (Nova Medical, Inc., Wilmington, MA). On the same day, MR imaging was also performed using a 3T whole-body MR system (Achieva 3.0 T; Philips) with an eight-channel head coil for reception (SENSE) and body coil for transmission.

The area of interest was 15 mm above and below the longitudinal axis of the corpus callosum. MT images were acquired using a 3D MT-prepared turbo field echo (MT-TFE) sequence.<sup>27,28</sup> Data were acquired first with off-resonance saturation (MT<sub>w</sub>; signal weighted by the MT effect) and second without saturation (MT<sub>nosat</sub>). The saturation was applied as a train of 20 off-resonance pulses (13.5  $\mu$ T Gaussian-windowed, sinc pulses with a bandwidth of 300 Hz, and off-resonance by  $\pm 1.05$  kHz [3.5 ppm], with 55 milliseconds between each pulse). The acquisition parameters were: field of view = 220  $\times$  220  $\times$  30 mm<sup>3</sup>; spatial resolution = .86  $\times$  .86  $\times$  1.5 mm<sup>3</sup>; echo time (TE) = 5.7 milliseconds; repetition time (TR) = 9.8 milliseconds; 20 slices; and total acquisition time 8:22 minutes. Figure 1 shows an example of MT<sub>w</sub> and MT<sub>nosat</sub> images. This study used MT<sub>w</sub> images (rather than MTR maps) as they had higher signal-to-noise ratio.

The acquisition parameters for 3T-2D-FLAIR sequence were: 256  $\times$  256 matrix; 50 interleave slices; spatial resolution 1  $\times$  1  $\times$  3 mm<sup>3</sup>; TE = 125 milliseconds; inversion time (TI) = 2,800 milliseconds; TR = 11,000 milliseconds; total acquisition time 5:52 minutes. The acquisition parameters for 7T-2D-FLAIR sequence were: 192  $\times$  192 matrix; 32 interleave slices; spatial resolution 1  $\times$  1  $\times$  4 mm<sup>3</sup>; TE = 100 milliseconds; TI = 2,800 milliseconds; TR = 15,000 milliseconds; and total acquisition time 6 minutes.

The scanning protocols included 3D T1-weighted magnetization-prepared rapid gradient-echo (MP-RAGE) imaging to assist with coregistering 3T-2D-FLAIR and 7T-3D-MT<sub>w</sub> images. Acquisition parameters at 7T were TE = 3.2 milliseconds; TR = 6.9 milliseconds; TI = 800 milliseconds; flip angle of the TFE readout pulse = 8°; TFE factor = 240; shot-to-shot interval = 8 seconds; spatial resolution = 1.25  $\times$  1.25  $\times$  1.25 mm<sup>3</sup>; field of view = 200  $\times$  200  $\times$  72.5 mm<sup>3</sup>; reconstruction matrix = 160  $\times$  160  $\times$  58; and total acquisition time 2 minutes.

### Image Analysis

#### Definition of Lesion

White matter lesions were defined as high signal intensity (SI) compared to background of white matter tissue not attributable to normal anatomical structures. Lesions were identified and marked using a consensus approach by two neurologists (IJC and RT) with experience in MRI analysis. They were blinded to patient identification and clinical information. The following were considered normal findings on FLAIR and MT<sub>w</sub> images: increased signal in a region of width  $\leq 2$  mm at the anterior and posterior pole of the lateral ventricles, increased signal in a strip of width  $\leq 2$  mm at the remainder of the lateral and third ventricles, symmetrically increased signal in the posterior limbs of the internal capsule, and any symmetric hyperintensity suggesting vessel, artifact, or anatomical structure.<sup>29,30</sup> If there was disagreement, a third neurologist (CSC) made the final consensus decision.

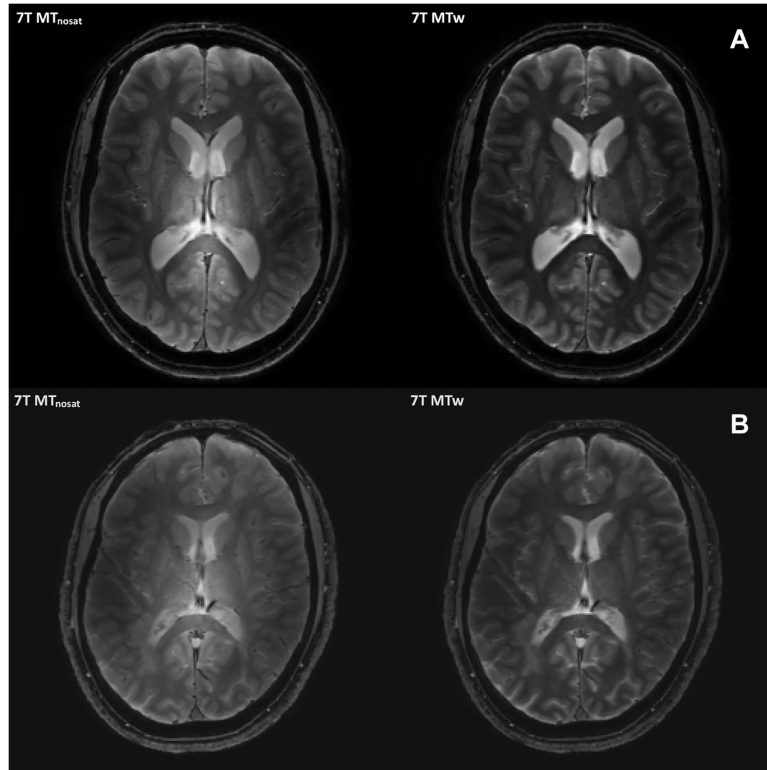


**Fig 1.** Axial 7-Tesla 3-dimensional MR images examples of magnetization transfer with no saturation pulse ( $MT_{nosat}$ ) and magnetization-transfer-weighted ( $MT_w$ ) in (A) a healthy subject and (B) a 27-year-old male patient with multiple sclerosis (score of the Expanded Disability Status Scale was 2.0).  $MT_w$  image (right) shows a better contrast of the gray matter to the white matter, and of white matter lesions to the normal appearing white matter than  $MT_{nosat}$  images (left).

#### *Imaging Postprocessing*

Acquired images were coregistered to the 3D-MP-RAGE image space using FLIRT linear rigid-body image registration algorithm from the FSL platform (FMRIB) ([www.fmrib.ox.ac.uk/fsl](http://www.fmrib.ox.ac.uk/fsl)).<sup>31</sup> Because of the difference in contrast between the original 7T-3D- $MT_w$  and 3T-2D-FLAIR scans and the reference scan, the cost function was the “mutual information” with a low number (100) of bins.

#### *Qualitative Assessment: Lesion Count*

The white matter lesions on 7T-3D- $MT_w$  images were manually compared to 3T-2D-FLAIR images by a single researcher (IJC). Figure 2 illustrates the images of the two-step analysis: first, we did an initial comparison between two images that were coregistered to the 3D MP-RAGE space. This step identified lesions in the same neuroanatomical region on both images. However, since the coregistered images were not perfectly in an alignment and were downsampled (Fig 2A), we then performed a retrospective comparison on original 3T-2D-FLAIR and 7T-3D- $MT_w$  images (Fig 2B).

#### *Quantitative Assessment: Lesion Load*

To determine the interrater agreement, images of two sequences were presented in random order to two neurologists (IJC and RT). The lesions were outlined using a semiautomated, seed-growing technique using NeuRoi software (Dr. CR Tench, Clinical Neurology, University of Nottingham, UK; <http://www.nottingham.ac.uk/scs/divisions/clinicalneurology/software/neuroi.aspx>). The total volume of these lesions was

calculated after manual segmentation. To evaluate intrarater reliability, all images were reassessed by IJC with a delay of  $\geq 1$  week to minimize any memory of the images.<sup>32</sup> An averaged lesion load derived from three assessments per subject was used for statistical analysis.

#### *Global Image Quality Assessment*

All images were evaluated by IJC. Image quality issues such as lesion detection, motion artifacts, and sharpness of all slices were rated 0–100, where 0 was perfect and 100 indicated the need to redo the scanning. Image quality was classified as excellent (0-30), good (30-70), or blurred (70-100).

#### *The Contrast for Lesions to Normal Appearing White Matter*

A total of 50 lesions were arbitrarily selected from different regions for estimation of the contrast between the SI from lesions and adjacent or contralateral normal-appearing white matter (NAWM). The percentage contrast between lesions and NAWM was calculated according to the following formula:  $\text{Contrast} = (SI_{\text{lesion}} - SI_{\text{NAWM}}) / (SI_{\text{lesion}} + SI_{\text{NAWM}}) \times 100$ .<sup>33</sup>

#### *Statistical Analysis*

Comparison between the subgroups was performed using Fisher’s exact test for dichotomized data and Mann-Whitney U test for continuous data or ordinal clinical rating scales. The analysis of brain lesions on the different sequences was performed patient-wise. The comparison of the numbers of lesions on 7T-3D- $MT_w$  versus 3T-2D-FLAIR was expressed as percentage gain or a loss in the number of detected brain lesions. The

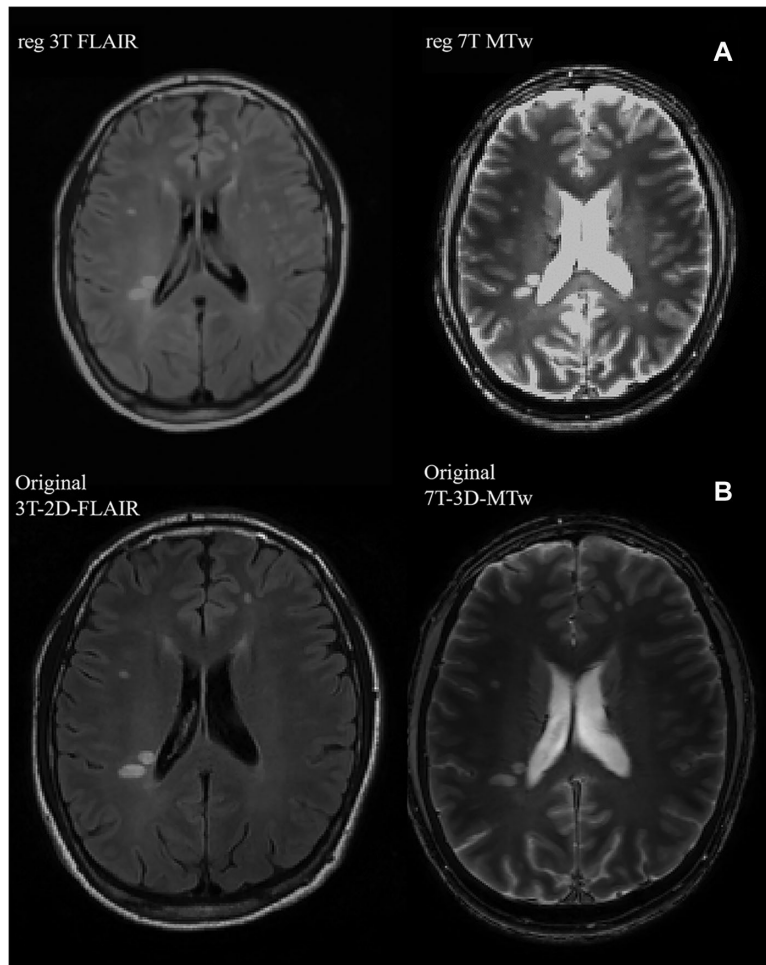


**Fig 2.** The two-step analysis. (A) Step 1: prospective assessment was done after 3-Tesla 2-dimensional-fluid-attenuated inversion recovery (3T-2D-FLAIR) or 7-Tesla 3-dimensional magnetization-transfer-weighted (7T-3D-MT<sub>w</sub>) was coregistered to the imaging space of 7-Tesla 3-dimensional magnetization-prepared rapid gradient echo (voxel dimension of 1.25 × 1.25 × 1.25 mm<sup>3</sup>). (B) Step 2: retrospective assessment was performed on the original 3T-2D-FLAIR images (pixel dimension of 1 × 1 mm<sup>2</sup>, thickness of 3 mm) and 7T-3D-MT<sub>w</sub> images (voxel dimension of .86 × .86 × 1.5 mm<sup>3</sup>). reg = registered.

interobserver agreement in measuring lesion volumes from both sequences was calculated using intraclass correlation coefficient (ICC) with two-sided 95% confidence interval (CI). Spearman's rank correlation was used for correlating lesion load at 3T-2D-FLAIR and 7T-3D-MT<sub>w</sub> with clinical scores (EDSS, FSS, or MSFC). The difference of lesion-to-NAWM contrast between two sequences was investigated using Student's *t*-test. The two-tailed *P*-value ≤.05 was considered as a statistically significant.

## Results

### Patient Characteristics

We included 15 CIS, 6 MS, and 10 healthy volunteers. Characteristics of these subjects are shown in Table 1. Overall, the mean age was 36 ± 10 years and 55% of patients were female. The age and gender were not statistically different between subgroups. The median EDSS score of patients was 2.5 (interquartile range [IQR], 1.5 to 3.0), median FSS 5.0 (IQR, 2.7 to 5.9), and median MSFC sum score .11 (IQR, -.36 to .42).

Table 1. Baseline Characteristics of Participants

	CIS (n = 15)	MS (n = 6)	Controls (n = 10)
Median age (IQR) (year)	39 (28-43)	34 (27-54)	35 (25-38)
Female (%)	10 (67%)	4 (67%)	3 (30%)
Median months of disease duration (IQR)	15 (8-24)	65 (28-168)*	n.a.
Median EDSS (IQR)	1.5 (1.0-3.0)	3.0 (3.0-3.5)*	n.a.
Median FSS (IQR)	4.2 (2.6-5.9)	5.3 (3.6-5.8)	n.a.
Median MSFC sum score (IQR)	-.12 (-.34 to .41)	.23 (-.42 to .43)	n.a.

CIS = clinically isolated syndrome; EDSS = Expanded Disability Status Scale; FSS = Fatigue Severity Scale; IQR = interquartile range; MS = multiple sclerosis; MSFC = Multiple Sclerosis Functional Composite; n = patient number; n.a. = not applicable.

\*Statistical significance (*P* < .05) between patients with CIS and MS.



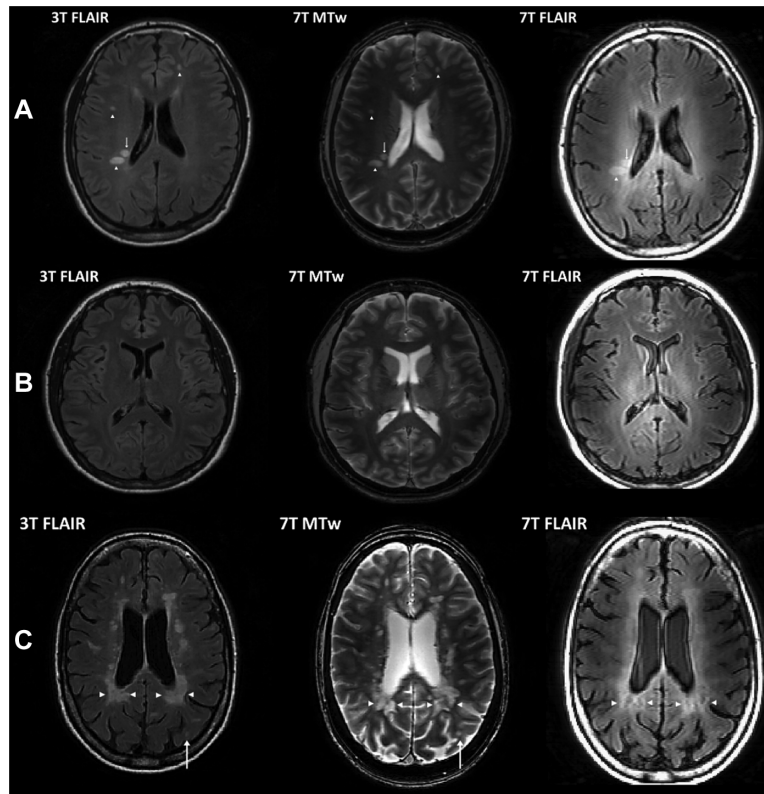


**Fig 3.** Axial 3-Tesla 2-dimensional-fluid-attenuated inversion recovery (3T-2D-FLAIR) (left), 7-Tesla 3-dimensional magnetization-transfer-weighted (7T-3D-MT<sub>w</sub>) (middle), and 7T-2D-FLAIR (right) in (A) a healthy participant; (B) a 40-year-old male with clinically isolated syndrome (score of the Expanded Disability Status Scale [EDSS] was 1.0) with discrete hyperintensities in the deep white matter (arrowhead) and periventricular white matter (arrow); and (C) a 56-year-old female with multiple sclerosis (score of EDSS was 6.5) with diffuse periventricular hyperintensities (arrowhead) and juxtacortical hyperintensities (arrow). The white matter lesion delineation is the least optimal on 7T-2D-FLAIR images.

### MRI Findings in Healthy Controls

Figure 3(A) shows an example of 3T-2D-FLAIR and 7T-3D-MT<sub>w</sub> images from a healthy participant. In eight healthy participants, nonspecific discrete hyperintensities were observed in periventricular and deep white matter regions. No diffuse periventricular hyperintensity or juxtacortical hyperintensity was found in the healthy volunteers.

### Sensitivity of White Matter Lesion Detection Using 7T MT<sub>w</sub> Images

Figure 3 shows examples of 3T-2D-FLAIR, 7T-3D-MT<sub>w</sub>, and 7T-2D-FLAIR images. The quality of lesion delineation of 7T-2D-FLAIR is lower than 3T-2D-FLAIR. Table 2 shows the sensitivity of lesion detection of 7T-3D-MT<sub>w</sub> compared to 3T-2D-FLAIR, and retrospective assessment enhances sensitivity compared to the initial assessment. Overall, 662 lesions were identified on original 3T-2D-FLAIR images, and 669 lesions on original 7T-3D-MT<sub>w</sub> images. Ten of 662 hyperintensities (1.5%) in 3T-2D-FLAIR images were not found retrospectively in the corresponding regions on 7T-3D-MT<sub>w</sub> images. Seventeen of 669 hyperintensities (2.5%) on 7T-3D-MT<sub>w</sub> images were not identified on 3T-2D-FLAIR images. Taking the 3T-2D-FLAIR images as the gold standard scan, we found a sensitivity of 98% (95% CI: 97% to 99%) for detecting lesions on the 7T-3D-MT<sub>w</sub> images. The sensitivity for detecting lesions on 7T-3D-MT<sub>w</sub> was 98% (95% CI: 96% to 99%) for CIS patients (318/325 lesions)

and 99% (95% CI: 98% to 100%) for MS patients (327/329 lesions).

The 27 lesions found by one scan type but not the other had a maximum diameter <3 mm (Fig 4). Hyperintensities observed in the basal ganglia on 3T-2D-FLAIR images were less distinguishable on the corresponding 7T-3D-MT<sub>w</sub> images (Fig 4A); most of the hyperintensities observed only on 7T-3D-MT<sub>w</sub> images were elongated in the through-plane direction, and possibly represented perivenous (Virchow-Robin) spaces.

### Intrarater and Interrater Reliability and Comparison of Lesion Loads

The mean lesion loads in healthy participants, CIS, and MS patients were 49, 4,996, and 15,102 mm<sup>3</sup> for 3T-2D-FLAIR and 24, 2,056, and 6,573 mm<sup>3</sup> for 7T-3D-MT<sub>w</sub>, respectively. The intrarater reliability was excellent: ICC was 96% (95% CI: 92% to 98%) for 3T-2D-FLAIR and 98% (95% CI: 97% to 99%) for 7T-3D-MT<sub>w</sub>. There was strong agreement between two neurologists: ICC of 98% (95% CI: 93% to 98%) for 3T-2D-FLAIR and 82% (95% CI: 66% to 91%) for 7T-3D-MT<sub>w</sub>. Lesion load in each sequence was highly correlated (correlation .910, *P* < .001) (Fig 5). Excluding healthy volunteers, the correlation coefficient was .875 (*P* < .001).

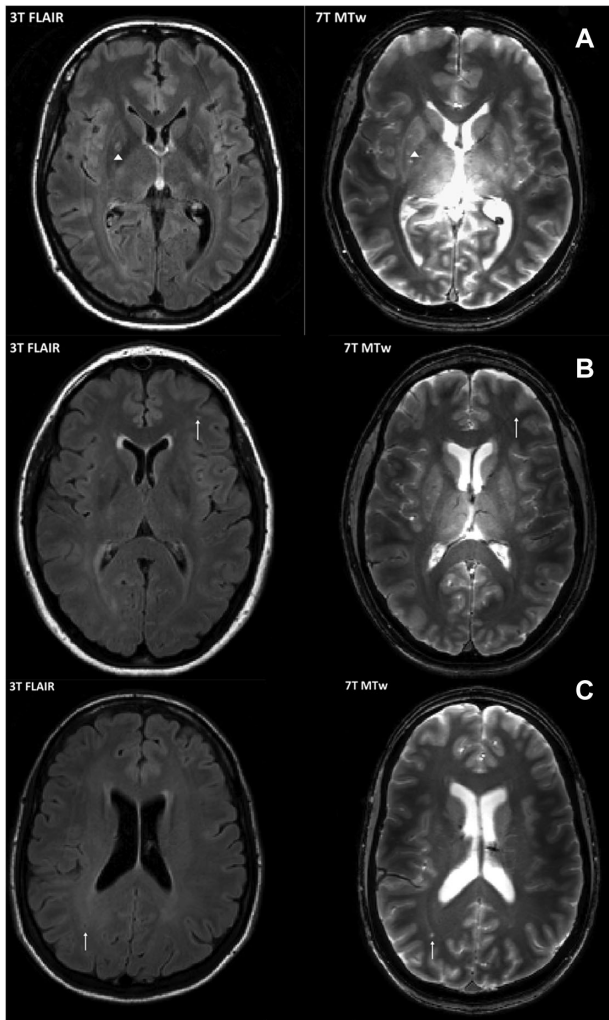
The quality of images was rated excellent (= 29, 94%) and good (*n* = 2, 6%) for both sequences. The lesion-to-NAWM

Table 2. Lesion Counts and Sensitivity of the Supratentorial Brain White Matter

Subjects	Prospective analysis on registered images				Retrospective analysis on original images			
	All (n = 31)	CIS (n = 15)	MS (n = 6)	Controls (n = 10)	All (n = 31)	CIS (n = 15)	MS (n = 6)	Controls (n = 10)
3T-2D-FLAIR	634	306	320	8	662	325	329	8
7T-3D-MT <sub>w</sub>	538	274	258	6	669	329	327	13
Seen on both images	505	250	249	6	652	318	327	7
Sensitivity (%) of 7T-3D-MT <sub>w</sub> using 3T-2D-FLAIR as the gold standard (95% confidence interval)	80 (76-83)	82 (77-86)	78 (73-82)	75 (35-97)	98 (97-99)	98 (96-99)	99 (98-100)	88 (47-100)

The two-step analysis for white matter lesions was applied on 3-Tesla 2-dimensional fluid-attenuated inversion recovery (3T-2D-FLAIR) and 7-Tesla 3-dimensional magnetization-transfer-weighted (7T-3D-MT<sub>w</sub>) images.

CIS = clinically isolated syndrome; MS = multiple sclerosis; n = patient number.



**Fig 4.** Comparison of discrete hyperintensities at the same neuroanatomical regions on axial 3-Tesla 2-dimensional-fluid-attenuated inversion recovery (3T-2D-FLAIR) images (left) and 7-Tesla 3-dimensional magnetization-transfer-weighted (7T-3D-MT<sub>w</sub>) images (right). (A) Observable lesion in the basal ganglia (arrowhead) on 3T-2D-FLAIR only; (B) observable lesion in the deep white matter on 3T-2D-FLAIR only (arrow); and (C) observable lesion (arrow) in the deep white matter on 7T-3D-MT<sub>w</sub> only.

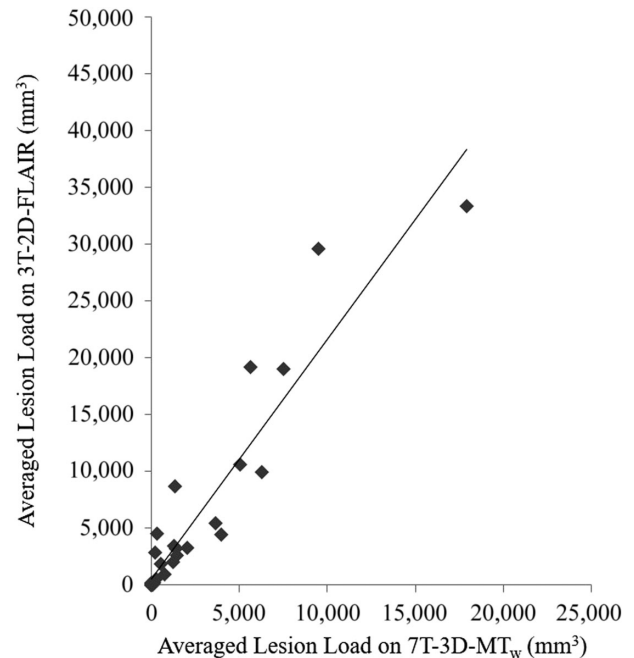


**Fig 5.** The linear association between lesion loads estimated by 3-Tesla 2-dimensional-fluid-attenuated inversion recovery (3T-2D-FLAIR) and by 7-Tesla 3-dimensional magnetization-transfer-weighted (7T-3D-MT<sub>w</sub>) images (Spearman Rank correlation, rho = .910, P < .001).

contrast for 7T-3D-MT<sub>w</sub> and 3T-2D-FLAIR images was comparable (mean ± standard deviation, 27 ± 9% vs. 26 ± 5%).

#### Clinical Correlation

In patients (n = 21), EDSS correlated with lesion load at 7T-3D-MT<sub>w</sub> (rho = .519, P = .016) and 3T-2D-FLAIR (rho = .496, P = .022). FSS score correlated with the lesion load at 7T-3D-MT<sub>w</sub> (rho = .506, P = .019) and 3T-2D-FLAIR (rho = .437, P = .048). MSFC sum or component scores did not correlate with lesion load.

#### Discussion

We assessed the performance of 7T-3D-MT<sub>w</sub> in detecting lesions seen on 3T-2D-FLAIR in patients with CIS or MS. Defining 3T-2D-FLAIR images as gold standard, we found that

7T-3D-MT<sub>w</sub> imaging could detect white matter lesions with 98% sensitivity. The correlation between the lesion loads and EDSS or fatigue was similar using both images. Therefore, our study supports a role for 7T-MT<sub>w</sub> for lesion detection in inflammatory demyelinating conditions. Of note, although lesion count on both sequences was similar, estimated lesion load on 3T-2D-FLAIR was almost twice that on 7T-3D-MT<sub>w</sub>. This may be related to the increased spatial resolution on 7T-3D-MT<sub>w</sub> (.86 × .86 × 1.5 mm<sup>3</sup>) versus 3T-2D-FLAIR (1 × 1 × 3 mm<sup>3</sup>). It may also reflect differences in contrast sensitivities, FLAIR being more sensitive to perilesional edema.<sup>34</sup>

Seven-Tesla MRI in MS or CIS is known to be safe and well tolerated,<sup>35</sup> and provides high-resolution visualization and quantification of disease-specific alterations, including myelin content.<sup>1,17,36–41</sup> MTR maps and MT<sub>w</sub> at 7T can be useful for detecting intracortical lesions compared to double inversion recovery (DIR) sequences at 3T.<sup>17</sup> Lesion visualization and volume estimation are better on MT<sub>w</sub> than MTR map. Because MTR represents ratios between MT sequences without and with saturation (MT<sub>nosat</sub> and MT<sub>w</sub>) sequentially, patient motion between the two sequences is not always avoidable. This study supports the use of 7T-MT<sub>w</sub> for lesion detection with high sensitivity compared to 3T-FLAIR with the additional benefit that the MT can be used to quantify the lesion myelin by calculating MTR (or even estimate the bound proton pool fraction through quantitative MT scanning) at the same scan session.

Seven-Tesla MRI can provide increased contrast and generate superior anatomical imaging and disease-specific lesion assessment compared to 3T.<sup>41,42</sup> However, it still presents challenges. Whereas T1- or T2\*-weighted scans are now widely used at 7T, T2-weighted FLAIR imaging remains limited, particularly for noncortical lesions, because of RF inhomogeneity effects and increased SAR, and lengthened gray and white matter T1 relaxation times (meaning that signals are not fully recovered at the inversion time when CSF signal is nulled). Despite efforts to overcome these issues, current FLAIR imaging at 7T shows variations in the transmit field causing regional hypointensity throughout the brain, particularly in the temporal lobes,<sup>43</sup> heterogeneous CSF suppression,<sup>22</sup> and long acquisition times.<sup>23</sup> Our study shows that while 3D-MT<sub>w</sub> imaging is technically more straightforward than 7T FLAIR, it shows similar white matter lesion detection rate to 3T-2D-FLAIR, while providing additional information on the myelin content,<sup>12</sup> useful for longitudinal or cross-sectional studies. MT<sub>w</sub> imaging did not detect 10 (1.5%) hyperintensities observed on 3T-2D-FLAIR images and detected 17 (2.5%) hyperintensities that were not visualized on 3T-2D-FLAIR. These minor differences may be attributed to the fact that MT<sub>w</sub> images have a smaller imaging resolution and the sequence is more sensitive to pathological changes related to macromolecular-bound protons than FLAIR images, as shown in brain abscesses<sup>44</sup> or tuberculoma.<sup>45</sup>

Some limitations of the current study deserve discussion. First, we only included supratentorial regions. Demyelinating lesions in MS or CIS occur most frequently in periventricular regions, and were captured in our study. The visibility of lesions in the temporal lobes and cerebellum needs further evaluation, as 7T transmit RF field inhomogeneity is high in these regions. Second, caution is needed in directly comparing estimates of lesion volumes on 3T-2D-FLAIR and 7T-3D-MT<sub>w</sub> images as acquisition and resolution were different. The acquisition protocol was 3D for 7T MT<sub>w</sub> and 2D for 3T FLAIR, with images

registered to 3D MP-RAGE images that may affect the results (eg, sensitivity to motion). The measured lesion load in 7T-3D-MT<sub>w</sub> correlated with EDSS and fatigue in a similar manner to that in 3T-2D-FLAIR, which is remarkable for this small number of patients. Third, the sample size was relatively small and most patients enrolled in this study, primarily aimed at exploring quantitative changes in early demyelinating disease, had short disease duration. However, for the purposes of validating 7T-3D-MT<sub>w</sub> for lesion detection and delineation, short duration is an advantage, fewer lesions being confluent. Fourth, we did not analyze cortical lesions, which require different but more sophisticated techniques.<sup>17</sup> Indeed, 7T FLAIR may be superior for cortical lesions.<sup>19</sup> Fifth, imaging inhomogeneity at 7T may be controlled to some extent by using multitransmit technology that was not available in this study. Furthermore, a direct comparison between 7T FLAIR and 7T MT<sub>w</sub> is desirable but at the time the optimized 7T FLAIR was not acquired for research quality analysis due to unresolved technical issues (mentioned above). Such a study in the future, using optimized 7T FLAIR, may well show this sequence to be more sensitive in detecting white matter lesions than both 7T MT<sub>w</sub> and 3T FLAIR. In the absence of such optimized 7T FLAIR, however, 7T MT<sub>w</sub> appears to be a reliable sequence for white matter lesions.

## Conclusions

MT<sub>w</sub> imaging at 7T allows evaluation and assessment of supratentorial lesions with similar white matter lesion detection to 3T FLAIR images in patients with CIS or MS. The results support the application of MT<sub>w</sub> imaging at 7T in the detection and volume estimation of demyelinating lesions as a reliable substitute for FLAIR imaging. However, a prospective study to compare white matter lesion detection between optimized 7T FLAIR, 7T MT<sub>w</sub>, and 3T FLAIR at the same imaging resolution and dimension will help determine the most sensitive sequence for white matter lesions at 7T.

## References

1. Mackenzie IS, Morant SV, Bloomfield GA, et al. Incidence and prevalence of multiple sclerosis in the UK 1990-2010: a descriptive study in the General Practice Research Database. *J Neurol Neurosurg Psychiatry* 2014;85:76-84.
2. Thompson AJ, Polman CH, Miller DH, et al. Primary progressive multiple sclerosis. *Brain* 1997;120:1085-96.
3. Polman CH, Reingold SC, Banwell B, et al. Diagnostic criteria for multiple sclerosis: 2010 revisions to the McDonald criteria. *Ann Neurol* 2011;69:292-302.
4. Popescu V, Agosta F, Hulst HE, et al. Brain atrophy and lesion load predict long term disability in multiple sclerosis. *J Neurol Neurosurg Psychiatry* 2013;84:1082-91.
5. Fisniku LK, Brex PA, Altmann DR, et al. Disability and T2 MRI lesions: a 20-year follow-up of patients with relapse onset of multiple sclerosis. *Brain* 2008;131:808-17.
6. Grossman RI, Gomori JM, Ramer KN, et al. Magnetization transfer: theory and clinical applications in neuroradiology. *Radiographics* 1994;14:279-90.
7. Schmierer K, Scaravilli F, Altmann DR, et al. Magnetization transfer ratio and myelin in postmortem multiple sclerosis brain. *Ann Neurol* 2004;56:407-15.
8. Wolff SD, Balaban RS. Magnetization transfer contrast (MTC) and tissue water proton relaxation in vivo. *Magn Reson Med* 1989;10:135-44.
9. Dousset V, Grossman RI, Ramer KN, et al. Experimental allergic encephalomyelitis and multiple sclerosis: lesion characterization with magnetization transfer imaging. *Radiology* 1992;182:483-91.



10. Brochet B, Dousset V. Pathological correlates of magnetization transfer imaging abnormalities in animal models and humans with multiple sclerosis. *Neurology* 1999;53:S12-7.
11. van Waesberghe JH, Castelijns JA, Lazeron RH, et al. Magnetization transfer contrast (MTC) and long repetition time spin-echo MR imaging in multiple sclerosis. *J Magn Reson Imaging* 1998;16:351-8.
12. Schmierer K, Tozer DJ, Scaravilli F, et al. Quantitative magnetization transfer imaging in postmortem multiple sclerosis brain. *J Magn Reson Imaging* 2007;26:41-51.
13. De Coene B, Hajnal JV, Gatehouse P, et al. MR of the brain using fluid-attenuated inversion recovery (FLAIR) pulse sequences. *AJNR Am J Neuroradiol* 1992;13:1555-64.
14. Kates R, Atkinson D, Brant-Zawadzki M. Fluid-attenuated inversion recovery (FLAIR): clinical prospectus of current and future applications. *Top Magn Reson Imaging* 1996;8:389-96.
15. Okuda T, Korogi Y, Shigematsu Y, et al. Brain lesions: when should fluid-attenuated inversion-recovery sequences be used in MR evaluation? *Radiology* 1999;212:793-8.
16. Simon JH, Li D, Traboulsee A, et al. Standardized MR imaging protocol for multiple sclerosis: Consortium of MS Centers consensus guidelines. *AJNR Am J Neuroradiol* 2006;27:455-61.
17. Abdel-Fahim R, Mistry N, Mougou O, et al. Improved detection of focal cortical lesions using 7T magnetisation transfer imaging in patients with multiple sclerosis. *Mult Scler Relat Disord* 2014;3:258-65.
18. Al-Radaideh A, Mougou OE, Lim SY, et al. Histogram analysis of quantitative T1 and MT maps from ultrahigh field MRI in clinically isolated syndrome and relapsing-remitting multiple sclerosis. *NMR Biomed* 2015;28:1374-82.
19. de Graaf WL, Kilsdonk ID, Lopez-Soriano A, et al. Clinical application of multi-contrast 7-T MR imaging in multiple sclerosis: increased lesion detection compared to 3 T confined to grey matter. *Eur Radiol* 2013;23:528-40.
20. van Veluw SJ, Fracasso A, Visser F, et al. FLAIR images at 7 Tesla MRI highlight the ependyma and the outer layers of the cerebral cortex. *Neuroimage* 2015;104:100-9.
21. Visser F, Zwanenburg JJ, Hoogduin JM, et al. High-resolution magnetization-prepared 3D-FLAIR imaging at 7.0 Tesla. *Magn Reson Med* 2010;64:194-202.
22. de Graaf WL, Zwanenburg JJ, Visser F, et al. Lesion detection at seven Tesla in multiple sclerosis using magnetisation prepared 3D-FLAIR and 3D-DIR. *Eur Radiol* 2012;22:221-31.
23. Saranathan M, Tourdias T, Kerr AB, et al. Optimization of magnetization-prepared 3-dimensional fluid attenuated inversion recovery imaging for lesion detection at 7T. *Invest Radiol* 2014;49:290-8.
24. Kurtzke JF. Rating neurologic impairment in multiple sclerosis: an expanded disability status scale (EDSS). *Neurology* 1983;33:1444-52.
25. Krupp LB, LaRocca NG, Muir-Nash J, et al. The fatigue severity scale. Application to patients with multiple sclerosis and systemic lupus erythematosus. *Arch Neurol* 1989;46:1121-3.
26. Fischer JS, Rudick RA, Cutter GR, et al. The multiple sclerosis functional composite measure (MSFC): an integrated approach to MS clinical outcome assessment. National MS Society Clinical Outcomes Assessment Task Force. *Mult Scler* 1999;5:244-50.
27. Mougou OE, Coxon RC, Pitiot A, et al. Magnetization transfer phenomenon in the human brain at 7 T. *Neuroimage* 2010;49:272-81.
28. Mougou O, Clemence M, Peters A, et al. High-resolution imaging of magnetisation transfer and nuclear Overhauser effect in the human visual cortex at 7T. *NMR Biomed* 2013;26:1508-17.
29. Neema M, Guss ZD, Stankiewicz JM, et al. Normal findings on brain fluid-attenuated inversion recovery MR images at 3T. *AJNR Am J Neuroradiol* 2009;30:911-6.
30. Molyneux PD, Tubridy N, Parker GJ, et al. The effect of section thickness on MR lesion detection and quantification in multiple sclerosis. *AJNR Am J Neuroradiol* 1998;19:1715-20.
31. Jenkinson M, Bannister P, Brady M, et al. Improved optimization for the robust and accurate linear registration and motion correction of brain images. *Neuroimage* 2002;17:825-41.
32. Molyneux PD, Tofts PS, Fletcher A, et al. Precision and reliability for measurement of change in MRI lesion volume in multiple sclerosis: a comparison of two computer assisted techniques. *J Neurol Neurosurg Psychiatry* 1998;65:42-7.
33. Sati P, George IC, Shea CD, et al. FLAIR\*: a combined MR contrast technique for visualizing white matter lesions and parenchymal veins. *Radiology* 2012;265:926-32.
34. Naganawa S. The technical and clinical features of 3D-FLAIR in neuroimaging. *Magn Reson Med Sci* 2015;14:93-106.
35. Chou JJ, Tench CR, Gowland P, et al. Subjective discomfort in children receiving 3T MRI and experienced adults' perspective on children's tolerability of 7T: a cross-sectional questionnaire survey. *BMJ Open* 2014;4:e006094.
36. Yao B, Ikonomidou VN, Cantor FK, et al. Heterogeneity of multiple sclerosis white matter lesions detected with T2\*-weighted imaging at 7.0 Tesla. *J Neuroimaging* 2015;25:799-806.
37. Blazejewska AI, Al-Radaideh AM, Wharton S, et al. Increase in the iron content of the substantia nigra and red nucleus in multiple sclerosis and clinically isolated syndrome: a 7 Tesla MRI study. *J Magn Reson Imaging* 2015;41:1065-70.
38. Mistry N, Dixon J, Tallantyre E, et al. Central veins in brain lesions visualized with high-field magnetic resonance imaging: a pathologically specific diagnostic biomarker for inflammatory demyelination in the brain. *JAMA Neurol* 2013;70:623-8.
39. Al-Radaideh AM, Wharton SJ, Lim SY, et al. Increased iron accumulation occurs in the earliest stages of demyelinating disease: an ultra-high field susceptibility mapping study in clinically isolated syndrome. *Mult Scler* 2013;19:896-903.
40. Sinnecker T, Mittelstaedt P, Dorr J, et al. Multiple sclerosis lesions and irreversible brain tissue damage: a comparative ultrahigh-field strength magnetic resonance imaging study. *Arch Neurol* 2012;69:739-45.
41. Tallantyre EC, Morgan PS, Dixon JE, et al. 3 Tesla and 7 Tesla MRI of multiple sclerosis cortical lesions. *J Magn Reson Imaging* 2010;32:971-7.
42. Tallantyre EC, Morgan PS, Dixon JE, et al. A comparison of 3T and 7T in the detection of small parenchymal veins within MS lesions. *Invest Radiol* 2009;44:491-4.
43. Zwanenburg JJ, Hendrikse J, Visser F, et al. Fluid attenuated inversion recovery (FLAIR) MRI at 7.0 Tesla: comparison with 1.5 and 3.0 Tesla. *Eur Radiol* 2010;20:915-22.
44. Mishra AM, Reddy SJ, Husain M, et al. Comparison of the magnetization transfer ratio and fluid-attenuated inversion recovery imaging signal intensity in differentiation of various cystic intracranial mass lesions and its correlation with biological parameters. *J Magn Reson Imaging* 2006;24:52-6.
45. Saxena S, Prakash M, Kumar S, et al. Comparative evaluation of magnetization transfer contrast and fluid attenuated inversion recovery sequences in brain tuberculoma. *Clin Radiol* 2005;60:787-93.